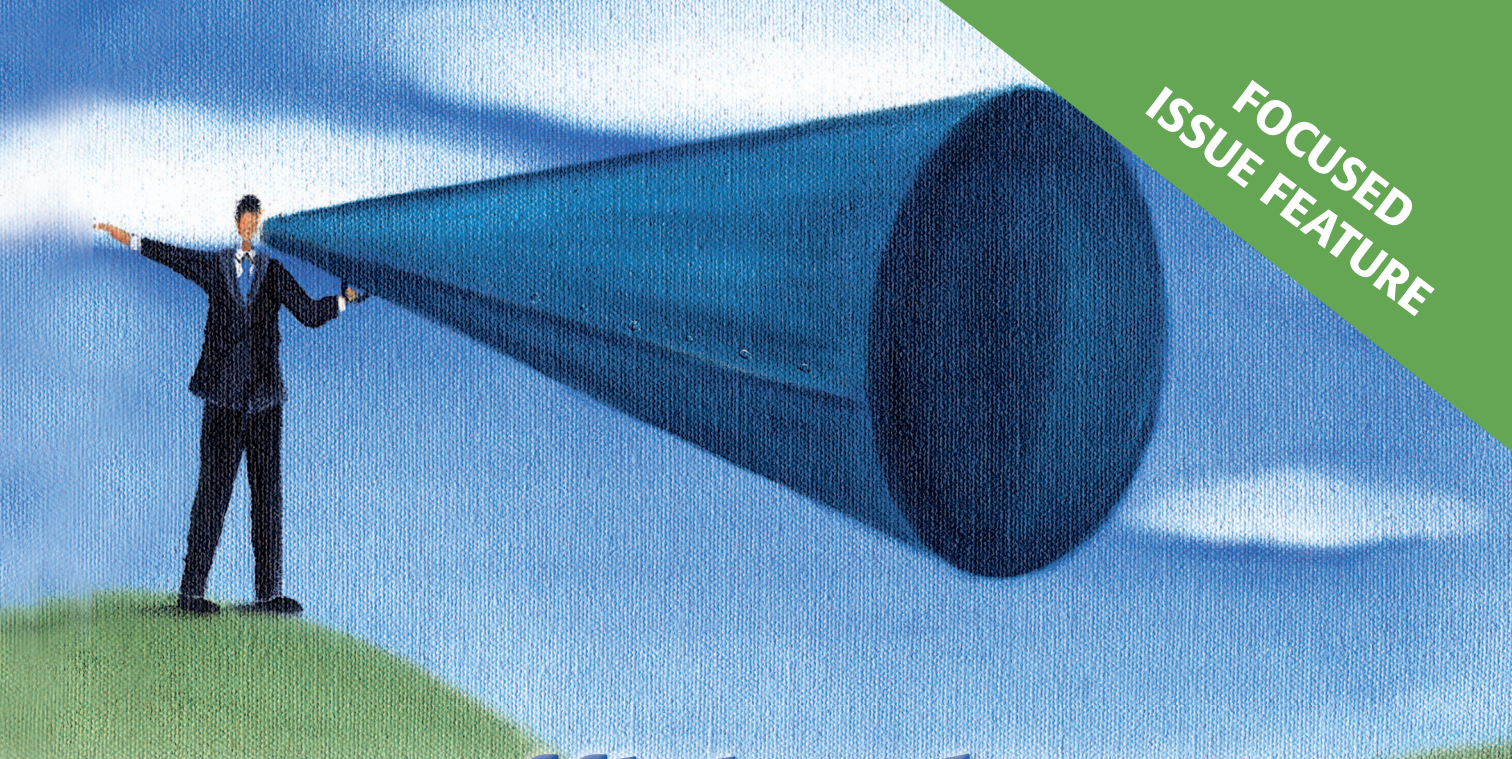

FOCUSED ISSUE FEATURE

Efficiently Amplified

Bumman Kim, Junghwan Moon, and Ildu Kim

Modern wireless communication systems have evolved to support increasing numbers of subscribers and provide higher data rate services within the limited frequency resources. As part of this evolution, many transmitted signals in the new standards, such as WCDMA, long term evolution (LTE), and worldwide interoperability for microwave access (WiMAX), now utilize a high peak-to-average power ratio (PAPR) caused by complex modulation schemes, generating the rapid change in the magnitude of signal as shown in Figure 1(a). In particular, as depicted in Figure 1(b), the PAPRs of the signals exceed 9 dB at 0.01% level of complementary cumulative distribution function. Use of high PAPR signals result in the power amplifier (PA) operating at a large enough back-off to satisfy the stringent linearity requirement. However, in this region, efficiency of the PA is very low. To bolster low efficiency in the back-off region, various efficiency boosting techniques have been considered over time. Recently, due to high-efficiency capabilities [1]–[13], supply voltage modulated PAs, such as envelope elimination and restoration (EER), hybrid-EER (H-EER), and envelope tracking (ET) technique,

Bumman Kim (bmkim@postech.edu), Junghwan Moon (jhmoon@postech.edu), and Ildu Kim are with the Department of Electrical Engineering, Pohang University of Science and Technology (POSTECH), Pohang, Republic of Korea.

Digital Object Identifier 10.1109/MMM.2010.937099

An important practical PA design problem is the nonlinear behavior of the output capacitance as a function of the supply voltage, which allows proper output matching only for a limited drain voltage range.

have received a lot of attention. Excellent experimental results have been reported using the various device technologies and modulated signals, as summarized in Table 1.

Figure 2 shows a dc power supply for a PA with and without the supply voltage modulation technique. While amplifying nonconstant-envelope modulated signals, the PA with a fixed supply voltage is adjusted for maximum power level and dissipates a lot of dc power at lower power, as shown in Figure 2(a). This inefficient operation consumes a lot of power internally and generates heat. Therefore, the transmitters require additional thermal management equipment to guarantee their reliability, which increases the cost and size of the systems. Figure 2(b) shows the concept of the supply modulated PA. Compared to PAs with fixed supply voltage, the dc supply is controlled appropriately to amplify the signal, and the dissipated power of the PA is minimized.

In this article, we briefly introduce supply modulated PAs, including the conventional EER, H-EER, and ET transmitters [1]–[17]. Much research on the supply modulated PA for base-station applications have been reported with excellent performance [6], [14]–[17]. However, those reports usually provide the implementation and experimental results using various device technologies, such as gallium nitride (GaN), laterally diffused MOS (LDMOS), and high voltage heterojunction bipolar transistor (HBT). In this article, we explain key design issues of PAs used for supply modulated PA transmitters. An important practical PA design problem is the nonlinear behavior of the output capacitance as a function of the supply voltage, which allows proper output matching only for a limited drain voltage range [6]–[8]. To minimize the impedance mismatch problem and maintain high efficiency for amplification of a signal with a high PAPR, the PA should be optimized in the high power generation region of the signal distribution [6], [8]. We also discuss another important design issue: suitable shaping method of the envelope voltage applied to PAs to solve linearity issues and achieve better power performance [8], [9]. In addition, losses in the supply modulator are considered. Finally, to provide an experimental comparison, the ET technique is applied to a Doherty amplifier [10], [11], illustrating how further enhanced performance can be obtained, in fact demonstrating the best performance among the many other good transmitters. These experimental results are included to clearly support our discussions, especially for base station applications.

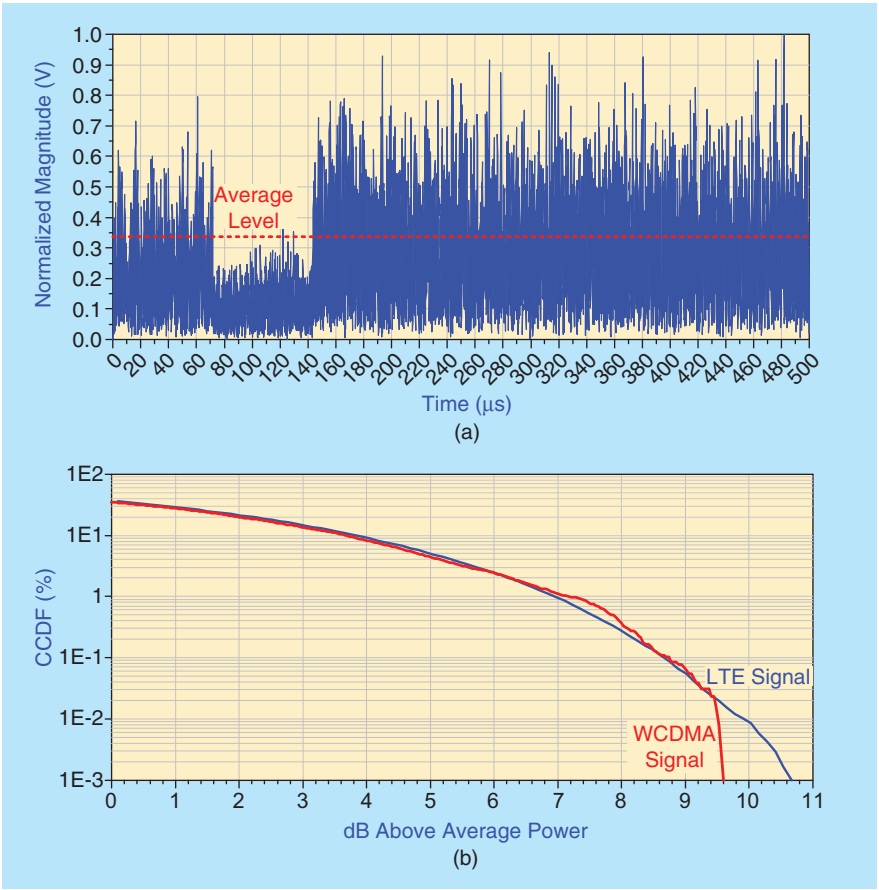

Figure 1. *(a) Time-domain waveform of a long-term evolution (LTE) signal. (b) Example complementary cumulative distribution functions (CCDFs) of WCDMA and long-term-evolution signals.*

Various Supply-Modulated Power Amplifiers

Dynamic power supply schemes include the EER, H-EER, and ET transmitters, classified according to the RF signal injected to the input of the PA and the supply voltage signal provided to the drain/collector bias of the PA. Detailed descriptions will be provided later.

TABLE 1. Summary of state-of-art envelope-tracking power amplifiers.

Ref.	DPD	Transistor	Signal	Output Power [W]	Efficiency [%]	PAE [%]	ACLR1/ ACLR2 [dBc]
[8]	Before DPD	GaN HEMT	2.655 GHz WiMAX 1FA 5 MHz 8.2 dB	19	44.4	40.9	−25.5 dB (RCE)
	After ML DPD			16	43.1	40.0	−33.6 dB (RCE)
[14]	Before DPD	GaN HFET	2.14 GHz WCDMA 1FA 3.84 MHz 7.67 dB	36.5	51.7	49.3	−32/−41
	After ML DPD			37.2	53.4	50.7	−48/−53
	After Memory DPD						−52/−58
[15]	Before DPD	LDMOS	2.14 GHz WCDMA 1FA 3.84 MHz 7.6 dB	26.9	40.8	40.3	−23/−44
	After ML DPD			27	40.9	40.4	−44/−53
	After Memory DPD						−54/−59
[16]	Before DPD	GaAs HVHBT	2.14 GHz WCDMA 1FA 3.84 MHz 7.7 dB	36.1	60	57	−36/−46
	After ML DPD			33.2	58	55	−48/−53
	After Memory DPD						−72/−70
	Before DPD		2.14 GHz WiMAX 10 MHz 8.8 dB	-	-	-	-
	After ML DPD			25	51	48	−41/−41
	After Memory DPD						−63/−62
[17]	Before DPD	GaAs HVHBT	2.14 GHz WCDMA 1FA 3.84 MHz 7.6 dB	-	-	-	-
	After ML DPD			29.76	-	54.15	−44.4/−53.18
	After Memory DPD			29.69	-	53.99	−55.39/−55.57

ML DPD: Memoryless digital predistortion, Efficiency: drain or collector efficiency of the ET PA
ACLR1: 5 MHz or 5.45 MHz offset for WCDMA or WiMAX signal, ACLR2: 10 MHz or 9.75 MHz offset for WCDMA or WiMAX signal

The supply modulated PA employs a high-efficiency switching-mode or linear amplifier together with a supply modulator. The supply modulator can be categorized into three types: 1) low dropout (LDO) regulator [18], 2) switched-mode power supply (SMPS) such as a dc-dc converter [19], [20], and 3) hybrid-switching amplifier (HSA) consisting of an SMPS and a class-AB amplifier [4]–[10], [12], [15]–[17], [21], [22]. Although the LDO linearly amplifies the supply voltage signal applied to the PA, it cannot provide sufficiently high efficiency for high PAPR signals such as orthogonal frequency division multiplexing (OFDM) and WCDMA. On the other hand, high efficiency is achieved by the SMPS. It converts the time-varying envelope signal to a binary pulse wave. This signal is then amplified and filtered to recover the input waveform. However, the available bandwidth is limited by the switching frequency because the efficiency of the SMPS is inversely proportional to the switching frequency. Even though the above mentioned topologies are employed for high-efficiency operation of the PA, they are not suitable for the base-station

Since PAs for the ET architecture operate at a higher supply voltage than that of the EER/H-EER transmitter, they provide higher output power over the whole input range, leading to increased gain.

applications, in which signals with a high PAPR and wide bandwidth are amplified.

Recently, the HSA has been widely used in supply modulated PAs to efficiently supply the drain voltage for base-station as well as handset applications. It uses a class-AB amplifier as a wide-bandwidth linear voltage source and the SMPS as a current source to provide a large portion of power at the low frequencies, achieving simultaneously high fidelity and efficiency. In this topology, the SMPS does not follow the load current with a high slew-rate any more, and it operates as a quasiconstant current source. The class-AB amplifier supplies and sinks the current to regulate the load according to the envelope signal. As a result, this architecture is suitable for envelope signals of modern wireless communications such that most supply modulated power amplifiers for base station applications employ this topology.

Envelope Elimination and Restoration Transmitters

The EER transmitter shown in Figure 3(a) theoretically presents very high efficiency over the entire power range with good linearity. The normal Cartesian $I(t)/Q(t)$ signal is converted to the polar signal $A(t)/\Phi(t)$. The RF phase information $\Phi(t)$, having a constant magnitude, is injected to the input of a high-efficiency PA and the amplitude information $A(t)$ is applied to the drain of the PA through the supply modulator. In this way, the amplitude information is recovered. The relationship between $I(t)/Q(t)$ and $A(t)/\Phi(t)$ can be expressed as follows:

$$A(t) = \sqrt{[I(t)]^2 + [Q(t)]^2}$$

$$\Phi(t) = e^{j\tan^{-1}\left(\frac{Q(t)}{I(t)}\right)}. \quad (1)$$

Since the original constellation is restored through the accurate recombination of the phase and amplitude information, it requires a fine-tuned time alignment of the phase and envelope paths.

In this architecture, since the input power of the PA is always a constant envelope signal containing the phase information only, it seems that there are no nonlinearities related to the variation of the input power, such as amplitude modulation-to-amplitude modulation (AM-to-AM) and amplitude modulation-to-phase modulation (AM-to-PM). However, the envelope is ideally recovered by the drain bias modulation, which can create many practical problems.

Although bias modulation leads to possible usage of highly efficient PAs with poor linearity for linear amplification, the constant envelope signal, whose level is enough to saturate the PA at high supply voltage level, with the phase information is too large to be useful at a low power level, leading to a low gain and power-added efficiency (PAE). It induces leakage from the input signal to the output signal and results in a nonlinear VDD-to-AM characteristic, as shown in Figure 4. Additionally, the equivalent circuit model of the PA is changed according to the supply voltage, and the output capacitance becomes the most important variable, generating a large phase distortion [23]. The phase signal has a wide bandwidth due to signal regrowth during the nonlinear conversion from the Cartesian to polar signal as described in (1), and creates a difficulty for the design of the PA. In

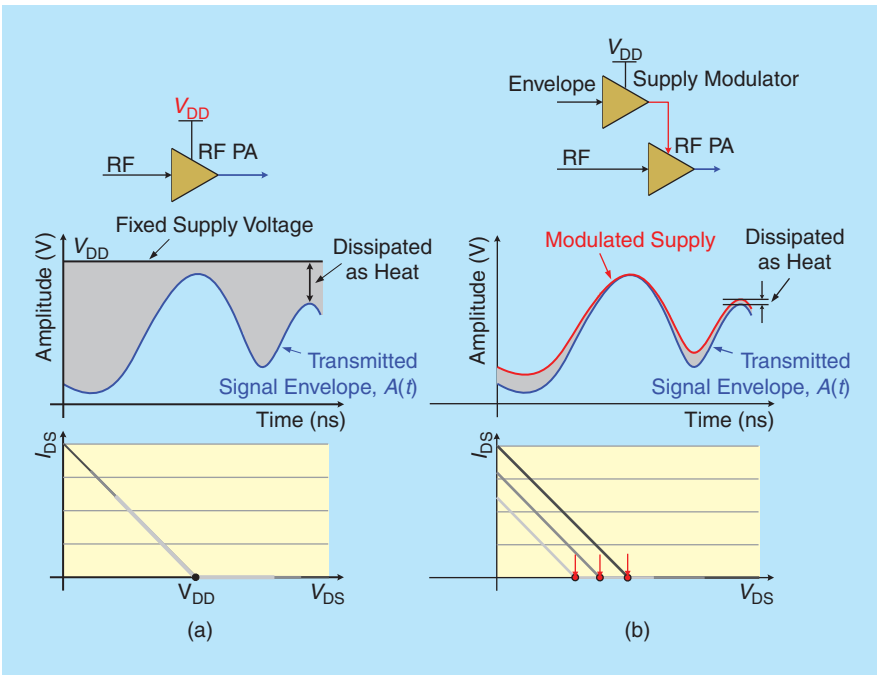

Figure 2. *(a) General power amplifier with a fixed supply voltage. (b) Concept of a supply-modulated power amplifier.*

general, the phase signal has a bandwidth several times wider than the baseband complex signal, as shown in Figure 5. Thus, to deliver high efficiency with good linearity, the PA should cover this wide bandwidth.

Traditionally, linear PAs such as class-AB amplifiers are utilized in ET transmitters to obtain good linearity with high efficiency [8].

Hybrid-EER Transmitters

To maintain the high efficiency of the EER transmitter and reduce the stringent requirements of time alignment and wide bandwidth, the H-EER architecture has been proposed, as depicted in Figure 3(b) [5], [7]. Although the supply voltage applied to the drain of the PA is still the envelope signal $A(t)$, the input of the PA is a complex-modulated signal in the H-EER transmitter. This alleviates the wide bandwidth requirements of the PA, increases the gain and PAE, and reduces the input leakage of the transmitter by reducing the input power. Moreover, the H-EER has lower sensitivity to the time mismatch between the envelope and RF paths than the conventional EER transmitter. However, the H-EER transmitter still has serious VDD-to-AM and VDD-to-PM nonlinearities in the low supply voltage region, as shown in Figure 4, because of its small transconductance characteristic and the rapid changes of the nonlinear components such as C_{DS} and C_{GD} in this region.

Envelope Tracking Transmitters

Figure 3(c) represents an ET transmitter system. Similar to that of an H-EER transmitter, the input signal of the PA is not a constant envelope signal with phase information but a complex-signal envelope. Thus, this transmitter has advantages of the H-EER transmitter, such as less precise time alignment between the envelope and RF paths. Moreover, unlike the conventional EER and H-EER schemes, the envelope signal injected into the PA is no longer the original envelope signal $A(t)$ extracted from $I(t)$ and $Q(t)$ but is adjusted for optimized performance.

An example of the envelope signal for the ET amplifier is shown in Figure 6. While the envelope signal of the EER/H-EER amplifier increases linearly, that of the ET transmitter does not. V_{offset} is equal to or greater than

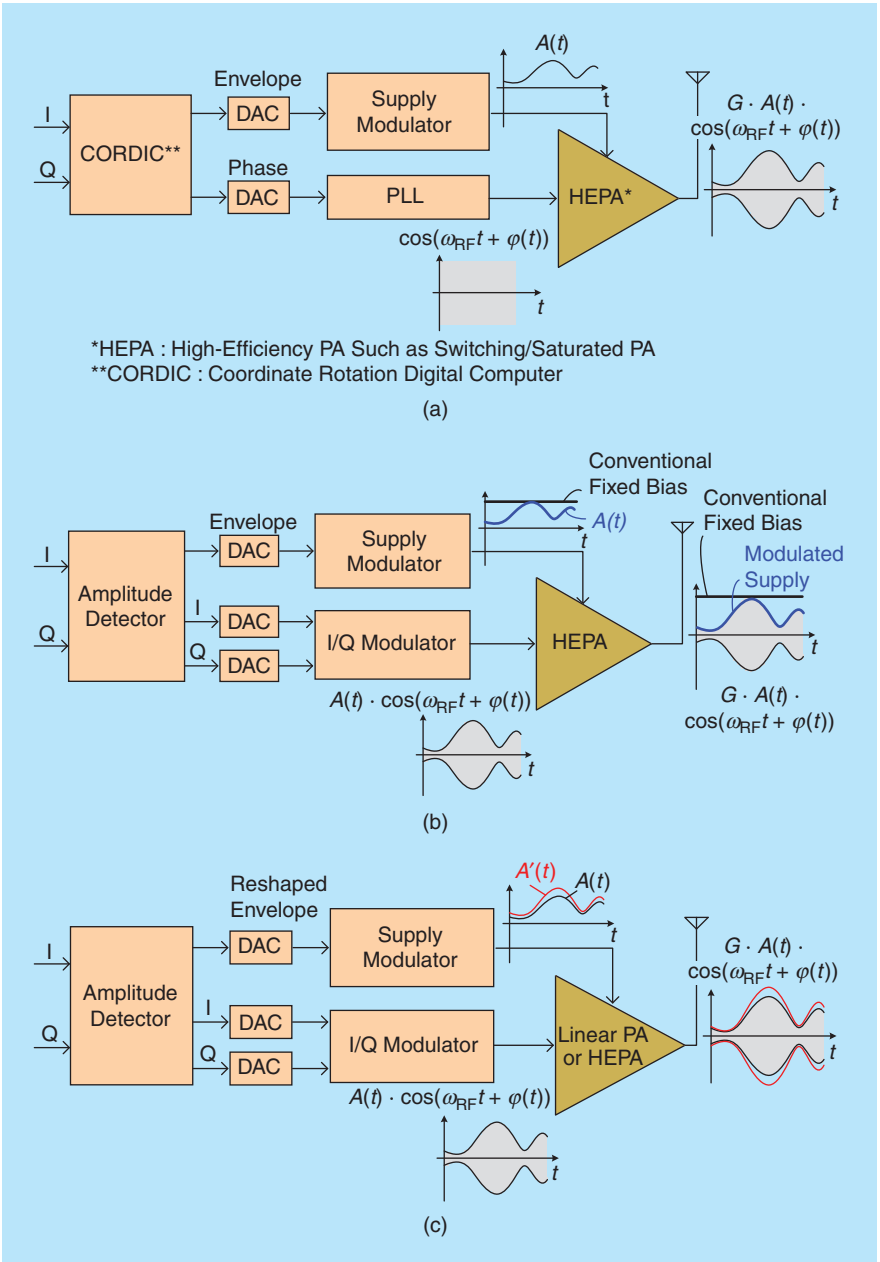

Figure 3. *(a) Block diagram of a conventional envelope elimination and restoration amplifier. (b) Block diagram of a hybrid-envelope-elimination and restoration amplifier. (c) Block diagram of an envelope-tracking transmitter.*

the knee voltage (the voltage at which the IDS curves transition from the linear region, where IDS depends on both VGS and VDS, to the saturation region, where IDS depends mainly on VGS and not VDS) of the power transistor to avoid operation in the strongly bias-dependent region. By operating above the knee voltage, the severely nonlinear behavior of the PA is prevented. In addition, since PAs for the ET architecture operate at a higher supply voltage than that of the EER/H-EER transmitter, they provide higher output power over the whole input range, leading to increased gain.

For high efficiency, PAs for the EER/H-EER and ET transmitters are operated in a saturated state for all envelope amplitudes applied to the PAs. Also, the PA for the ET operation has higher efficiency than the EER/H-EER transmitter because of the reduced knee voltage effect and nonlinear capacitance impedance mismatch. Traditionally, linear PAs such as class-AB amplifiers, are utilized in ET transmitters to obtain good linearity with high efficiency [8].

Design of Power Amplifiers for Supply-Modulated Transmitters

In general, amplifiers employed in supply-modulated transmitters are designed to provide maximum efficiency at the peak supply voltage. In this case, the output capacitance is dependent on the drain voltage, and output is significantly impedance mismatched at low-voltage regions, degrading the output power and efficiency. The average efficiency of the supply-modulated PA depends on the probability density function (PDF) of the complex-modulated

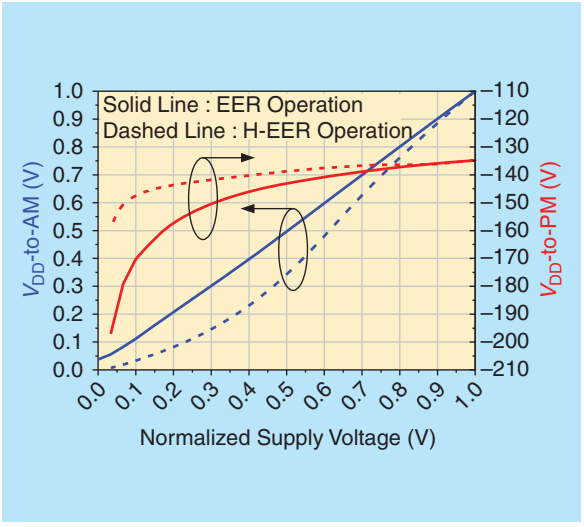

Figure 4. *Amplitude modulation and phase modulation distortion of the supply voltage under envelope elimination and restoration and hybrid envelope elimination and restoration operations. These are extracted for a saturated power amplifier using a GaN high-electron mobility transistor.*

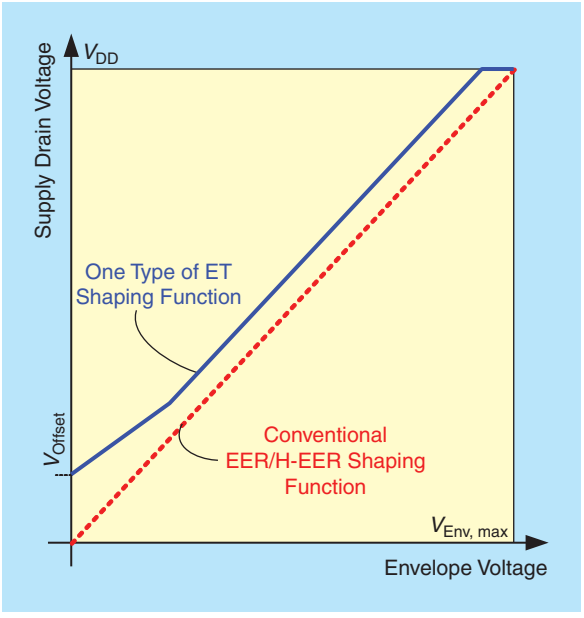

Figure 6. *Shaping functions for the supply voltage for envelope elimination and restoration/hybrid envelope elimination and restoration and envelope tracking transmitters.*

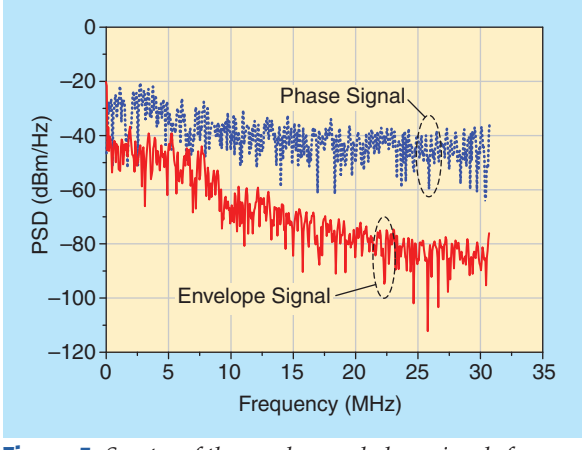

Figure 5. *Spectra of the envelope and phase signals for the long-term evolution 1FA signal, having a bandwidth of 10 MHz.*

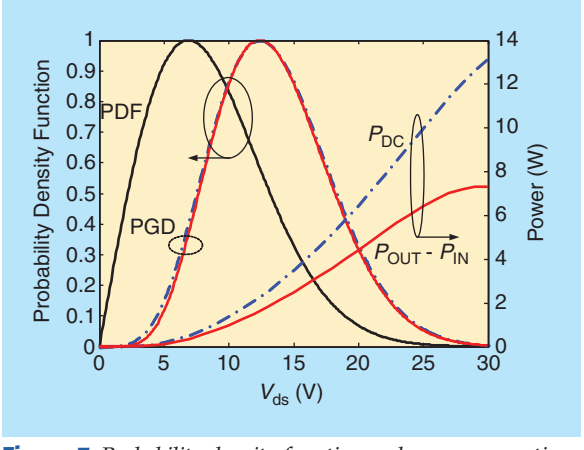

Figure 7. *Probability density function and power generation distribution of the WCDMA signal with peak-to-average power ratio of 9.8 dB.*

input signal because the supply voltage applied to the amplifier follows the PDF [6], [7]. The average PAE of the supply tracked transmitter can be derived as follows:

$$\mathrm{PAE} = \frac{\int \mathrm{PDF}(V_{\mathrm{ds}}) \cdot [P_{\mathrm{out}}(V_{\mathrm{ds}}) - P_{\mathrm{in}}(V_{\mathrm{ds}})] dV_{\mathrm{ds}}}{\int \mathrm{PDF}(V_{\mathrm{ds}}) \cdot P_{\mathrm{dc}}(V_{\mathrm{ds}}) dV_{\mathrm{ds}}}, \quad (2)$$

where P_{out} and P_{in} are the instantaneous output and input powers of the PA at a given V_{ds}. In this equation, the overall PAE is determined by ratio of integrals for the power-generation distribution, which is given by the multiplication of the PDF with the power factor $(P_{\mathrm{out}} - P_{\mathrm{in}})$ and PDF with P_{dc}.

Figure 7 illustrates the PDF, dc (blue dot-dash line), and RF (red solid line) power-generation distribution of a WCDMA signal having the PAPR of 9.8 dB when the maximum envelope voltage is 30 V. The peak value of the power-generation distribution appears at a higher value than that of the PDF. Even though maintaining a high efficiency over a wide range of drain bias is desired for the ET transmitter, it is challenging to keep the high efficiency over all ranges due to the dependence of the output capacitance on the drain voltage [24]. Therefore, the RF PA should be optimized for efficiency at the maximum power-generation distribution region. This means the output capacitance is tuned out at this region, resulting in the improved performance. For WCDMA signals with 9.8 dB PAPR, the maximum value of the distribution is located at 7 V, but that of the power-generation distribution is found at 12 V [7].

The time-delay between envelope and RF paths causes distortion in all of the supply modulated PAs. Therefore, it is crucial to minimize the time-mismatch to minimize the nonlinearity.

To illustrate these effects, the matching impedance variations due to nonlinear capacitances in the ET circuit are simulated using an inverse class-F amplifier [LDMOS field-effect transistor (LDMOSFET) MRF281SR1] at 1 GHz and depicted in Figure 8. In general, the harmonic load impedances for the inverse class-F are open and short for even and odd harmonics, respectively. Practically speaking, however, the harmonic control up to third order is enough to obtain high-efficiency operation. Thus, we have manipulated the harmonic contents up to the third harmonic.

Figure 8(a) and (b) shows the impedances seen at the output load for the PA designed at the 30 V and 12 V supply voltages, respectively. As shown in Figure 9(a), although the PA designed at 30 V provides the loadline (the plot of the current flow from current source of a device into the load and voltage across the load, where I can be easily plotted on the dc-IV plane, and from where we can see the nonzero current and voltage profiles, whose multiplication is the power dissipation in the transistor) of quasi-L shape (no nonzero overlap between the current and voltage, resulting in no internal power consumption and the highly efficient operation), it could not achieve the desired L

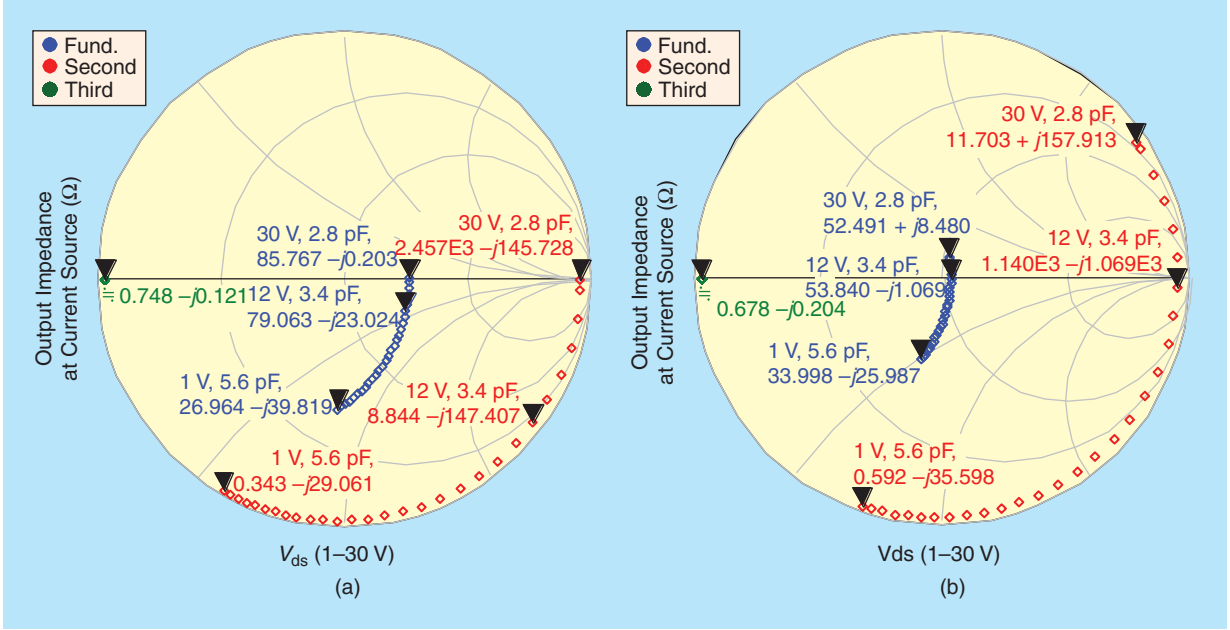

Figure 8. *Fundamental and harmonic load impedances versus V_{ds} of the MRF281SR1 laterally diffused MOSFET. (a) Power amplifier optimized at 30 V. (b) Power amplifier optimized at 12 V.*

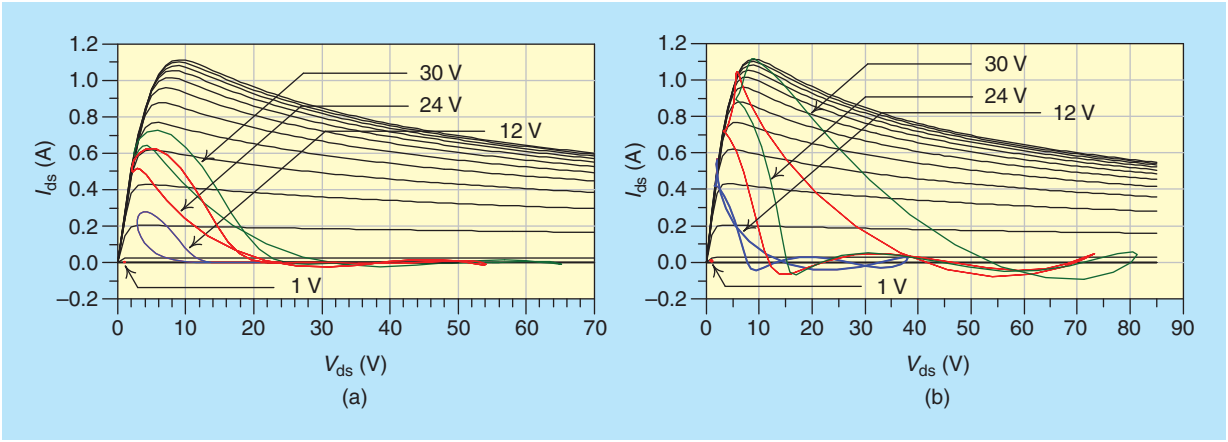

Figure 9. *(a) Loadlines of the power amplifiers, optimized at 30 V. (b) Loadlines of the power amplifiers, optimized at 12 V.*

shape around 12 V supply voltage due to the impedance mismatch caused by the nonlinear output capacitor. On the other hand, the amplifier optimized at 12 V delivers the inverse class-F operation, as depicted in Figure 9(b).

Using the designed PAs, the performance under the H-EER operation for a signal with a PAPR of 9.8 dB is evaluated by MATLAB. The simulation results are summarized in Table 2, where the average high-efficiency PA (HEPA) and peak high-efficiency PA denote the PAs optimized at 12 V and 30 V, respectively. The results clearly show that the PA should be optimized at the maximum power-generation distribution region to achieve the best performance under the drain supply-voltage modulation. Though all simulations are conducted under H-EER operation, the methodology for optimizing the PA at the maximum power-generation distribution region is also useful to increase performance of any supply-modulated transmitter architecture.

In addition to the design issues for maximizing PAE of the PA, the supply voltage injected into the drain/collector of the PA should be carefully shaped to maximize the performance of the supply modulated PA. This is because the nonlinear behavior of the output capacitance and transconductance, when the supply voltage changes, causes an impedance mismatch, nonuniform gain, and phase distortion. This results in poor AM-to-AM and AM-to-PM characteristics. As an example of envelope shaping, Figure 6 shows the drain bias modulation signals for the conventional H-EER and optimized ET transmitters. Unlike the conventional H-EER transmitter, the supply voltage shaping function for the ET amplifier has two different slopes with an offset voltage. The offset voltage in the low Vin region is adjusted to be higher than the power device's knee voltage. Through the operation above the knee region, PA operation in the severe nonlinear region can be avoided, reducing the gain compression and serious phase distortion generated in the low V_{in} region. Furthermore, the PA for the ET transmitter operates at a higher V_{ds} over the whole input power range when compared to that of the H-EER transmitter. Accordingly, the PA delivers higher output power over the whole input range, increasing the power gain. Later, we will experimentally demonstrate this behavior.

Additionally, since the overall PAE of the supply modulated PA is determined by not only the amplifier but also the supply modulator, it is important to reduce losses in the supply modulator. In particular, conduction and switching losses of the switch in the SMPS, voltage drop across the sensing resistor, and current sinking of the class-AB amplifier degrade the efficiency. Thus, careful design should be carried out to maximize efficiency of the HSA. To reduce losses of the SMPS, the size of the switch is carefully selected by balancing the conduction loss and the discharging loss of the switch. Moreover, switching speed should be optimized. If the switching speed increases, SMPS provides most of the current needed for the PA, reducing the current supply from the class-AB amplifier, which is good. However, increasing the switching speed creates a switching loss problem. In addition, power loss across the sensing resistor can be reduced by

TABLE 2. Calculated average performance by using MATLAB simulation for WCDMA 1FA signal having 9.8 dB PAPR.

	Output Power [dBm]	Input Power [dBm]	Gain [dB]	DE [%]	PAE [%]
Average HEPA	29.92	17.71	12.21	72.25	67.90
Peak HEPA	26.25	14.18	12.07	65.19	61.13

minimizing the value of resistor. Based on the above approaches, we demonstrate a maximized efficiency of the HSA.

Measurement Examples

To illustrate the design issues described above, the HSA as depicted in Figure 10 was designed and implemented. The detailed operating waveforms in each node of the HSA are shown in Figure 11. As the input signal V_{in} increases, current from the linear amplifier linearly increases, which is proportional to the sensing current. The sensed current is converted to the voltage V_{sen} , and it is directly applied to the input of the hysteretic comparator. At t_1, V_{sen} then becomes larger than the positive hysteresis voltage and the output of the comparator changes its state from 0 to 1, turning on the switch and increasing the current from the switching amplifier i_{sw} with the slope of $(V_{dd} - V_{out})/L$ during ΔT_1. As i_{sw} increases, i_{linear} decreases and V_{sen} is also decreased. At t_2, V_{sen} becomes smaller than the negative hysteresis voltage, and the output of the comparator is changed from 1 to 0. The switch is turned off, resulting in the decrease of i_{sw} with the slope of $2V_{out}/L$ during ΔT_2. Continuing this type of operation, the high-efficiency switching amplifier provides most of the current required to the load, while the wideband linear amplifier compensates for the switching-current ripple.

Experiments are carried out to demonstrate: 1) better performance of the average high-efficiency PA than the peak high-efficiency PA by accounting for the nonlinear output capacitance, and 2) the importance of bias shaping for the supply-modulated amplifier for ET transmitter.

As mentioned previously, the time-delay between envelope and RF paths causes distortion in all of the supply modulated PAs. Therefore, it is crucial to minimize the time-mismatch to minimize the nonlinearity. In the experiments, synchronization is carried out using delay tap in the Agilent ADS simulator and delay

In a real design environment, the nonlinear output capacitance depending on the supply voltage is one of the important design considerations. It prevents the amplifier from achieving a high PAE over the whole supply voltage range.

cable. In particular, time delay results in the asymmetric spectrum emission. As such, the delay adjustment is conducted in direction of reducing the unbalance of the output spectrum.

The better performance of the average high-efficiency PA under the H-EER operation is verified using the inverse class-F amplifier implemented in LDMOSFET at 1 GHz [7]. Two amplifiers are optimized at 30 V Vds and at maximum power-generation distribution region, 12 V Vds, respectively. The H-EER transmitter has been evaluated with a single-carrier WCDMA signal with a 3.84-MHz bandwidth and 9.8-dB PAPR. Measured results of the transmitter are summarized in Table 3. The H-EER transmitter using the PA optimized at the peak region has an output power of 29.2 dBm with an overall drain efficiency (DE) of 38.4%, and its overall PAE is 35.5% with a gain of 11.2 dB. On the other hand, the transmitter using the average high-efficiency PA has 2.5 dB more output power with efficiency of 41.2%, enhanced by 6.5%. Output spectra of H-EER transmitters are presented in Figure 12, showing that adjacent channel leakage ratio [(ACLR), indicating a measurement of the

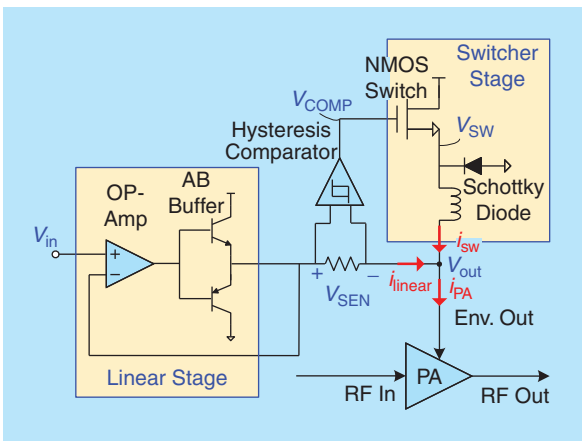

Figure 10. *Configuration of the implemented supply modulator.*

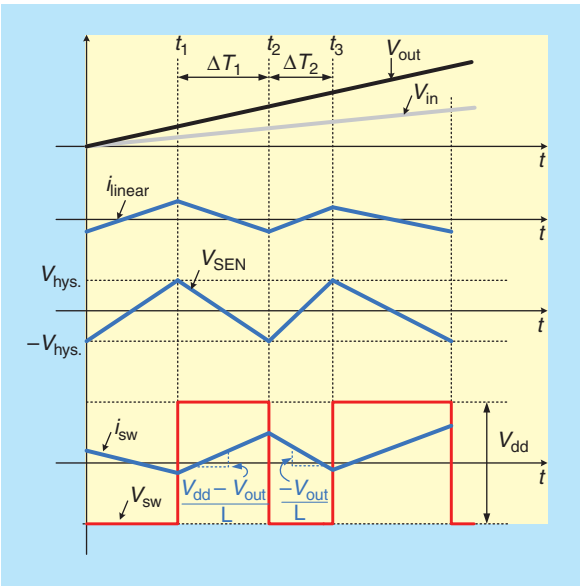

Figure 11. *Operating waveforms of the hybrid switching amplifier.*

TABLE 3. Summarized performance of the H-EER transmitters with PAs optimized at the peak and average supply voltage regions.

	Peak Region	Average Region
Output Power	29.19 dBm	31.71 dBm
Gain	11.19 dB	10.81 dB
Overall Drain Efficiency	38.42%	44.9%
Overall PAE	35.5%	41.18%
ACLR @ 5-MHz	−32.2 dBc	−35.7 dBc
ACLR @ 10-MHz	−41.9 dBc	−47.6 dBc
Error Vector Magnitude*	10.9%	6.4%

* Error vector magnitude is a measure of how far the signal constellation points are localized from the ideal locations at the Cartesian coordinate.

amount of power in the adjacent frequency channel, usually defined as the ratio of the average power in the adjacent frequency channel (or offset) to the average power in the transmitted frequency channel] for the average tuning is lower that of the other case. The better ACLR of the average high-efficiency PA is mainly caused by the compensation of the nonlinear output capacitance at the maximum power generation distribution (PGD) region, resulting in the smaller phase variation. The ACLRs are 235.7 dBc and 247.6 dBc at 5- and 10-MHz offsets, respectively. These experimental results clearly show the advantages of the amplifier optimized at the maximum power-generation distribution region.

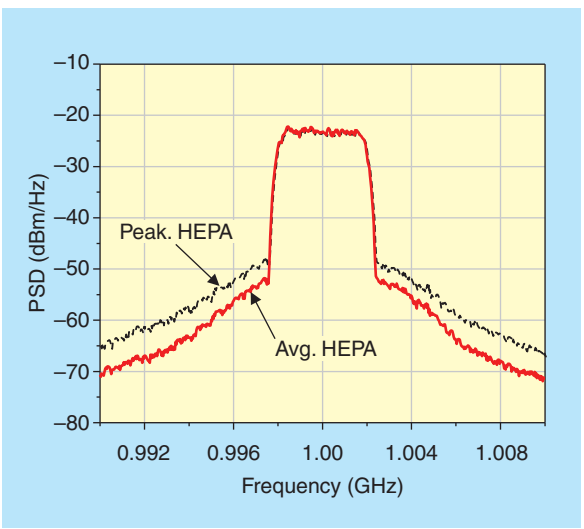

Figure 12. *Measured output spectra of the hybrid envelope elimination and restoration transmitter with the power amplifiers optimized at the peak and average supply voltage regions.*

As mentioned previously, the shape of the envelope signal injected into the PA is another important design factor. Figure 13(a) shows shaping functions of the drain bias modulation signals for the conventional H-EER and optimized ET transmitters. For high efficiency, both PAs for the H-EER and ET transmitters are operated at a saturated state for all values of the drain bias modulation signal. The PA for the ET operation has higher efficiency than the H-EER transmitter due to the reduced knee effect and impedance mismatch caused by the nonlinear capacitance. Consequently, enhanced overall PAE performance can be achieved by the ET technique [8]. The slope and offset voltage of the drain bias modulation signal for ET operation is adjusted for minimum spurious emission and high PAE performance at an improved output power, which is an optimized operation of the conventional H-EER transmitter.

To compare further the ET and H-EER techniques, we study the effect of voltage-supply modulation on a high-electron mobility transistor (HEMT) device. Based on the shaping method in Figure 13(a), the DE, PAE, output power, and gain are described for two modes of operation using a

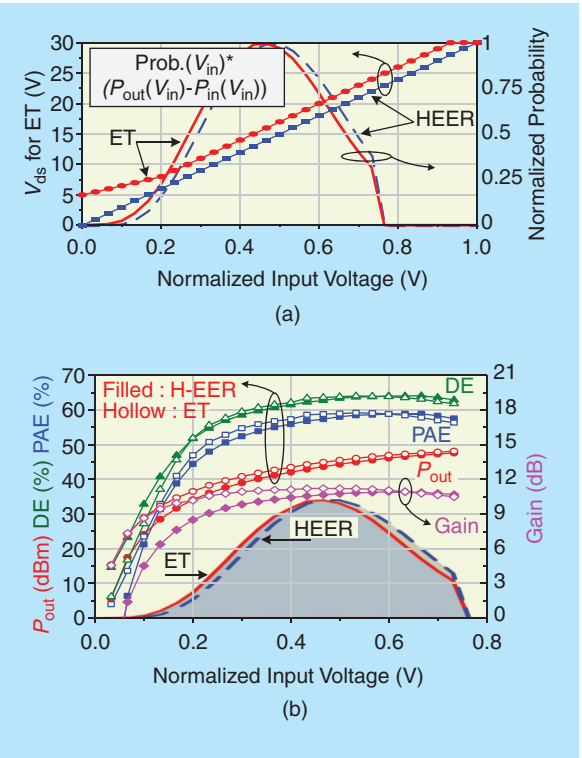

Figure 13. *(a) Shaping functions of the supply voltage signals and power generation distributions of the hybrid envelope elimination and restoration and envelope tracking transmitters. (b) Measured performance for a continuous wave signal under the hybrid envelope elimination and restoration and envelope tracking operations.*

TABLE 4. Summarized performance of the H-EER and ET transmitters for IEEE 802.16e mobile WiMAX signal.

	H-EER	ET
Output Power	42.3 dBm	42.8 dBm
Gain	10.1 dB	11 dB
Overall PAE	39.5%	40.9%
Relative Constellation Error*	−21.2 dB	−25.5 dB

* Relative constellation error (dB) = 20*log10(EVM).

continuous wave (CW) signal as shown in Figure 13(b). The PA used for measurement is designed using a GaN HEMT NPT25100 for a WiMAX 1FA signal with 5 MHz signal bandwidth and 8.2 dB PAPR at 2.655 GHz. Table 4 represents the measured results for the transmitter when the envelope signals described in Figure 13(a) are applied. The ET transmitter has achieved 40.9% PAE performance at an average output power of 42.8 dBm with 225.5 dB of relative constellation error (RCE). The measured output spectra are depicted in Figure 14. The measurement results demonstrate that the ET transmitter with optimized supply voltage shape is superior to the conventional H-EER transmitter.

Advanced Supply-Modulated Power Amplifier: The Doherty Envelope Tracking Transmitter

We next present a design example showing how a high-power amplifier can be implemented using the supply-modulated techniques described above. Currently, the Doherty PA and EER/ET transmitter are the most popular architectures, providing high efficiency over high instantaneous dynamic range for the signals required for modern wireless communication systems. The operation of the Doherty amplifier has been well documented in the literature [25]–[27]. Even though the Doherty amplifier shows good efficiency at the back-off power level, its high efficiency is maintained only to around the 6 dB back-off region. In EER/ET architectures, the efficiency drop at low supply voltages and insufficient efficiency of the supply modulator for high crest factor signals limit high-efficiency operation for wide instantaneous power ranges.

To overcome the disadvantages of each transmitter, the Doherty PA assisted by the supply modulator was introduced as an advanced supply modulated PA [10], [11]. Figure 15 shows a block diagram of the Doherty ET transmitter. Since the carrier amplifier generates most of the RF power for the modulation signal, it is not effective to modulate the supply voltage of the peaking amplifier. Thus, the carrier PA is modulated using the properly reshaped envelope signal. Modulating the supply voltage of the carrier amplifier for the Doherty amplifier mainly boosts the efficiency of the amplifier in the low-power region.

Since the supply voltage is modulated from the 6 dB back-off level, high efficiency in the high power region is achieved from the load modulation characteristic of the Doherty amplifier. It provides an extended dynamic range of 6 dB. Moreover, since only the supply voltage of the carrier amplifier is modulated from the 6 dB back-off level, the PAPR of the supply voltage amplified by the hybrid switching amplifier is reduced by 6 dB, as illustrated in Figure 16 [10].

The efficiency of hybrid switching amplifiers is closely related to PAPR of the input signal, and is lower for high PAPR signals. The modulation scheme used in the Doherty amplifier significantly enhances the efficiency of the supply modulator because the envelope signal injected into the carrier PA has 6 dB lower PAPR than conventional one, as shown in Figure 17. Thus, improved efficiency

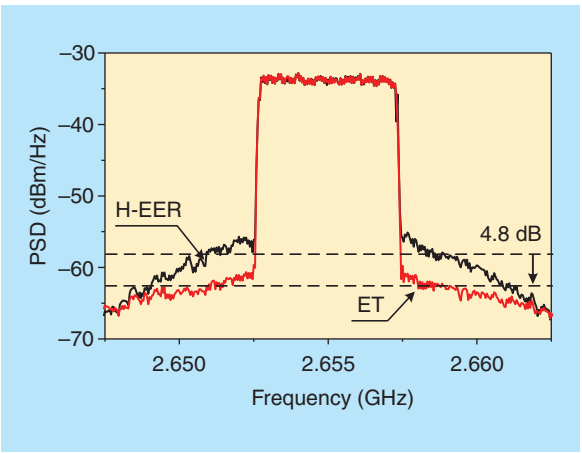

Figure 14. *Measured output spectra of the hybrid envelope elimination and restoration and envelope tracking transmitters.*

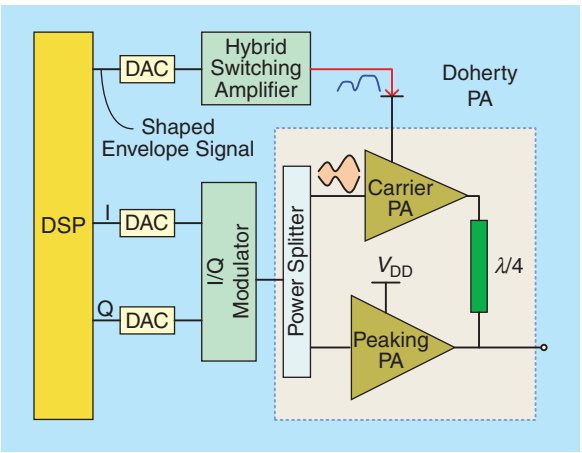

Figure 15. *Block diagram of the Doherty amplifier with supply modulator.*

These results clearly show that the polar transmitter with the saturated Doherty amplifier is the most promising architecture for highly efficient PAs.

results in better transmitter performance because the efficiency of the supply modulator is directly related to the overall efficiency of the supply-modulated PA. This relation is confirmed by MATLAB simulation with a WCDMA 1FA signal having a crest factor of 8 dB.

Although the Class-B amplifier with an ideal ET-modulator delivers the maximum efficiency for the whole power level range, the Doherty amplifier shows a slightly degraded efficiency at the high power region because only the carrier PA is supported by the supply modulator. However, together with the real supply modulator, the overall efficiency of the ET Doherty transmitter is better than that of the conventional EER as depicted in Figure 17. Because the envelope signal is injected into the carrier amplifier with the PAPR reduced by 6 dB, the supply modulator efficiency is significantly improved. Compared to the efficiency of the supply modulator for the Class-B amplifier, the efficiency is enhanced by more than 15% at the same average output power level over the broad output power range, as shown in Figure 17. This investigation shows the ET Doherty amplifier consisting of a saturated PA is a suitable transmitter architecture for highly efficient operation across a broad power range.

The Doherty architecture and supply modulator was implemented and optimized to demonstrate the high-efficiency capability [11]. The standalone Doherty amplifier is designed at 2.14 GHz using GaN HEMT CGH40010. As a unit cell PA of the Doherty structure, saturated amplifiers are employed to provide higher efficiency over a broad output power range compared to the general Doherty PA [28]. The Doherty amplifier shows a very high PAE for a WCDMA 1FA signal with a 8 dB PAPR. At the maximum average output power level, backed-off by 8 dB from the peak power, a PAE of 49.7% is obtained.

For the Doherty ET PA, only the supply voltage of the carrier amplifier is tracked. For the average output power back-off level from 0 to 6 dB, the applied envelope signal to the carrier amplifier is the same as shaping function #1 in Figure 16. Below the 6 dB back-off level, the offset voltage V_{offset} and the maximum value are increased, following #2 shaping, to avoid the severe gain reduction and achieve a good PAE. The designed saturated ET Doherty amplifier provides a PAE of 50.9% at the maximum average output power while those of the standalone saturated PA, saturated Doherty PA, and ET transmitter employing saturated PAs are 35.0%, 49.7%, and 42.3%, respectively, at the same average output power back-off level, and the results are summarized in Table 5. For a broad range of the average output power level, the PAE of the Doherty ET transmitter is better than those of other PAs, as depicted in Figure 18(a). For the ET transmitter with the saturated PA, the envelope signal applied to the PA is shaped by the shaping function #2, as shown in Figure 16. Figure 18(b) shows the measured ACLRs of the implemented PAs. These results clearly show that the polar transmitter with the saturated Doherty amplifier is the most promising architecture for highly efficient PAs.

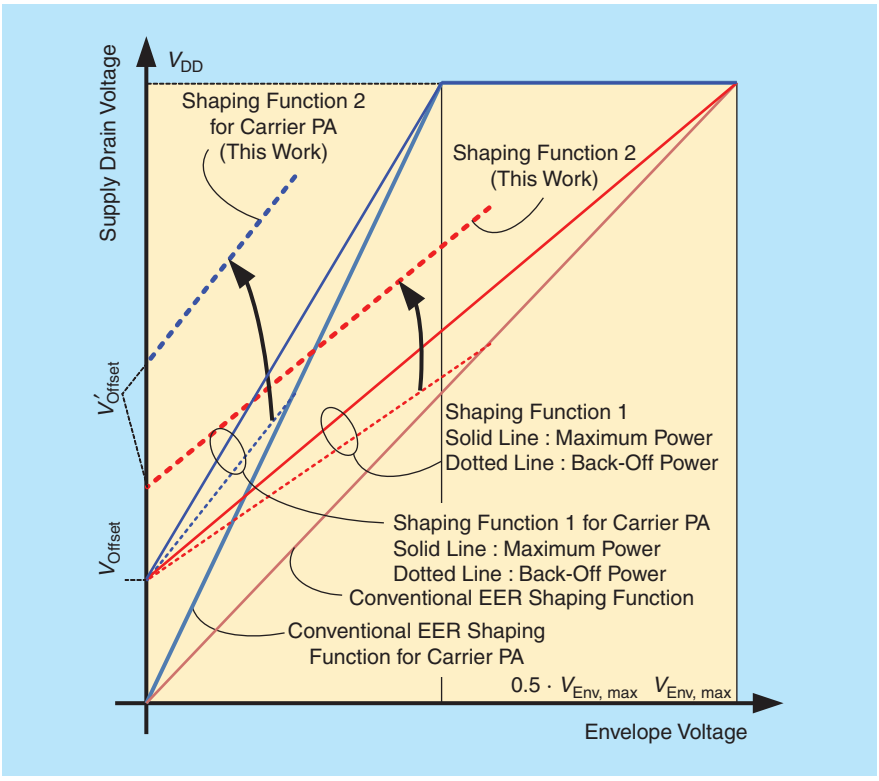

Figure 16. *Transfer functions of the envelope shaping functions for the carrier power amplifier and standalone power amplifier.*

Conclusion

In this article, a general overview and practical design methods for supply-modulated

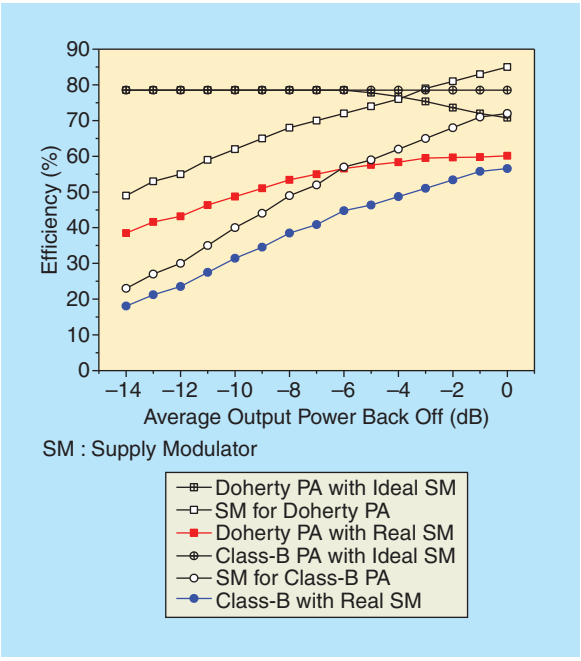

Figure 17. *Estimated efficiencies of the envelope tracking Doherty and conventional envelope elimination and restoration transmitters using ideal and real supply modulators for a WCDMA 1FA signal.*

transmitters were presented. Disadvantages of the conventional EER transmitter were discussed, such as wideband sensitivity to the time alignment between envelope and RF path, power leakage caused by excessive input power at low supply voltage, and poor PAE. This motivated the introduction of the H-EER transmitter, in which the input to the PA is a complex-modulated RF up-converted signal. The ET transmitter was presented to obtain better performance by injecting the optimum envelope signal to the PA.

TABLE 5. Performance summary at maximum average output power backoff level.

	PAE	ACLR
Sat. PA	35.0	−37.2
Sat. PA + ET	42.3	−27.0
Doherty	49.7	−24.5
Doherty + ET	50.9	−26.5

In a real design environment, the nonlinear output capacitance depending on the supply voltage is one of the important design considerations. It prevents the amplifier from achieving a high PAE over the whole supply voltage range. The work presented here illustrates that the average efficiency of the supply-modulated transmitter strongly depends on the power-generation distribution of the input signal. Thus, the PA in the transmitter should be designed for high performance over the maximum power-generation distribution region. Experimentally, this was demonstrated by comparing the average high-efficiency PA and peak high-efficiency PA in the transmitter. An ET amplifier with an optimized supply voltage was implemented and shown to provide better performance over the conventional H-EER transmitter.

Finally, to compensate for the drawbacks of the Doherty and supply-modulated PAs, a high-power transmitter consisting of a Doherty amplifier assisted by supply modulation was proposed

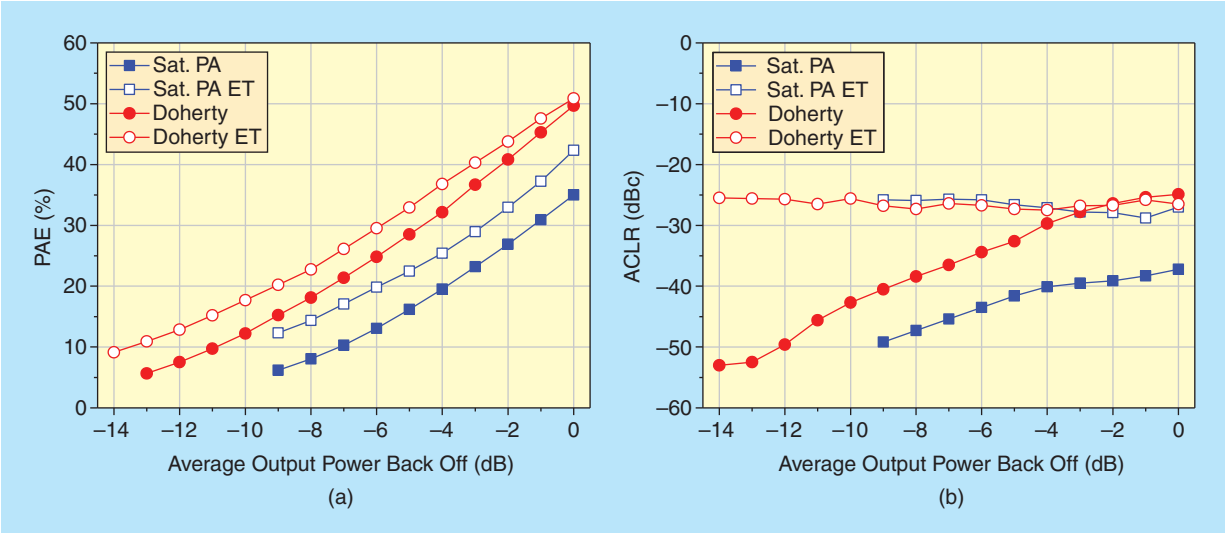

Figure 18. *(a) Measured power-added efficiency of the standalone Doherty and saturated power amplifiers, envelope tracking Doherty power amplifier and saturated envelope tracking power amplifier for a WCDMA 1FA signal at an offset frequency of 5 MHz. (b) Measured adjacent-channel leakage ratio performance of the standalone Doherty and saturated power amplifiers, envelope-tracking Doherty power amplifier and saturated envelope-tracking power amplifier for a WCDMA 1FA signal at an offset frequency of 5 MHz.*

and optimized. Its superior performance over conventional ET and Doherty amplifiers was experimentally demonstrated.

Acknowledgment

The authors would like to thank to Cree Inc. for providing the GaN HEMT transistors used in this work. This work was supported by the MKE (The Ministry of Knowledge Economy), Korea, under the ITRC (Information Technology Research Center) support program supervised by the NIPA (National IT Industry Promotion Agency)(NIPA-2010-(C1090-1011-0011)) and WCU(World Class University) program through the Korea Science and Engineering Foundation funded by the Ministry of Education, Science and Technology (Project No. R31-2008-000-10100-0).

References

[1] F. H. Raab, P. Asbeck, S. Cripps, P. B. Kenington, Z. B. Popovic, N. Pothecary, J. F. Sevic, and N. O. Sokal, "Power amplifiers and transmitters for RF and microwave," *IEEE Trans. Microwave Theory Tech.*, vol. 50, no. 3, pp. 814–826, Mar. 2002.

[2] L. Kahn, "Single-sideband transmission by envelope elimination and restoration," *Proc. IRE*, vol. 40, no. 7, pp. 803–806, July 1952.

[3] S. C. Cripps, *RF Power Amplifiers for Wireless Communications*. Norwood, MA: Artech House, 2006.

[4] F. Wang, D. F. Kimball, J. D. Popp, A. H. Yang, D. Y. C. Lie, P. M. Asbeck, and L. E. Larson, "Wideband envelope elimination and restoration power amplifier with high efficiency wideband envelope amplifier for WLAN 802.11g applications," in *IEEE MTT-S Int. Microwave Symp. Dig.*, June 2005, pp. 645–648.

[5] F. Wang, D. F. Kimball, J. D. Popp, A. H. Yang, D. Y. C. Lie, P. M. Asbeck, and L. E. Larson, "An improved power-added efficiency 19-dBm hybrid envelope elimination and restoration power amplifier for 802.11g WLAN applications," *IEEE Trans. Microwave Theory Tech.*, vol. 54, no. 12, pp. 4086–4099, Dec. 2006.

[6] D. F. Kimball, J. Jeong, C. Hsia, P. Draxler, S. Lanfranco, W. Nagy, K. Linthicum, L. E. Larson, and P. M. Asbeck, "High-efficiency envelope tracking W-CDMA base-station amplifier using GaN HFETs," *IEEE Trans. Microwave Theory Tech.*, vol. 54, no. 11, pp. 3848–3856, Nov. 2006.

[7] I. Kim, Y. Y. Woo, J. Kim, J. Moon, J. Kim, and B. Kim, "High-efficiency hybrid EER transmitter using optimized power amplifier," *IEEE Trans. Microwave Theory Tech.*, vol. 56, no. 11, pp. 2582–2593, Nov. 2008.

[8] I. Kim, J. Kim, J. Moon, and B. Kim, "Optimized envelope shaping for hybrid EER transmitter of mobile WiMAX Optimized ET operation," *IEEE Microwave Wireless Compon. Lett.*, vol. 14, no. 8, pp. 389–391, Aug. 2004.

[9] J. Choi, D. Kim, D. Kang, and B. Kim, "A polar transmitter with CMOS programmable hysteretic-controlled hybrid switching supply modulator for multistandard applications," *IEEE Trans. Microwave Theory Tech.*, vol. 57, no. 7, pp. 1675–1686, July 2009.

[10] J. Choi, D. Kang, D. Kim, and B. Kim, "Optimized envelope tracking operation of Doherty power amplifier for high efficiency over an extended dynamic range," *IEEE Trans. Microwave Theory Tech.*, vol. 57, no. 6, pp. 1508–1515, June 2009.

[11] J. Moon, J. Son, J. Kim, I. Kim, S. Jee, Y. Y. Woo, and B. Kim, "Doherty amplifier with envelope tracking for high efficiency," in *IEEE MTT-S Int. Microwave Symp. Dig.*, Anaheim, CA, May 2010.

[12] J. H. Chen, K. U-yen, and J. S. Kenney, "An envelope elimination and restoration power amplifier using a CMOS dynamic power supply circuit," in *IEEE MTT-S Int. Microwave Symp. Dig.*, June 2004, vol. 3, pp. 1519–1522.

[13] J. Choi, D. Kang, D. Kim, J. Park, B. Jin, and B. Kim, "Power amplifiers and transimitters for next generation mobile handset," *J. Semicond. Technol. Sci.*, vol. 9, no. 4, pp. 14–23, Dec. 2009.

[14] D. Kimball, P. Draxler, J. Jeong, C. Hsia, S. Lanfranco, W. Nagy, K. Linthicum, L. Larson, and P. Asbeck, "50% PAE WCDMA basestation amplifier implemented with GaN HFETs," in *Proc. Compound Semiconductor Integrated Circuit Symp.*, Oct. 2005, pp. 89–92.

[15] P. Draxler, S. Lanfranco, D. Kimball, C. Hsia, J. Jeong, J. van de Sluis, and P. Asbeck, "High efficiency envelope tracking LDMOS power amplifier for W-CDMA," in *IEEE MTT-S Int. Microwave Symp. Dig.*, San Francisco, CA, June 2006, pp. 1534–1537.

[16] D. Kimball, M. Kwak, P. Draxler, J. Jeong, C. Hsia, C. Steinbeiser, T. Landon, O. Krutko, L. Larson, and P. Asbeck, "High efficiency WCDMA envelope tracking base-station amplifier implemented with GaAs HVHBTs," in *Proc. IEEE Compound Semiconductor Integrated Circuit Symp.*, Monterey, CA, Oct. 2008, pp. 1–4.

[17] J. Jeong, D. F. Kimball, M. Kwak, C. Hsia, P. Draxler, and P. M. Asbeck, "Wideband envelope tracking power amplifiers with reduced bandwidth power supply waveforms and adaptive digital predistortion techniques," *IEEE Trans. Microwave Theory Tech.*, vol. 55, no. 12, pp. 2757–2765, Dec. 2007.

[18] P. Raynaert and S. Steyaert, "A 1.75-GHz polar modulated CMOS RF power amplifier for GSM-EDGE," *IEEE J. Solid-State Circuits*, vol. 40, no. 12, pp. 2598–2608, Dec. 2005.

[19] V. Pinon, F. Hasbani, A. Giry, D. Pache, and C. Garnier, "A singlechip WCDMA envelope reconstruction LDMOS PA with 130 MHz switched-mode power supply," in *IEEE Int. Solid-State Circuits Conf. Tech. Dig.*, Feb. 2008, pp. 564–565.

[20] P. Hazucha, G. Schrom, J. Hahn, B. A. Bloechel, P. Hack, G. E. Dermer, S. Narendra, D. Gardner, T. Karnik, V. De, and S. Borkar, "A 233-MHz 80%-87% efficient four-phase dc–dc converter utilizing air-core inductors on package," *IEEE J. Solid-State Circuits*, vol. 40, no. 4, pp. 838–845, Apr. 2005.

[21] F. Wang, D. F. Kimball, D. Y. Lie, P. M. Asbeck, and L. E. Larson, "A monolithic high-efficiency 2.4-GHz 20-dBm SiGe BiCMOS envelope tracking OFDM power amplifier," *IEEE J. Solid-State Circuits*, vol. 42, no. 6, pp. 1271–1281, June 2007.

[22] W. Chu, B. Bakkaloglu, and S. Kiaei, "A 10 MHz-bandwidth 2 mV-ripple PA-supply regulator for CDMA transmitters," in *IEEE Int. Solid-State Circuits Conf. Tech. Dig.*, Feb. 2008, pp. 448–449.

[23] J. C. Pedro, J. A. Garcia, and P. M. Cabral, "Nonlinear distortion analysis of polar transmitters," *IEEE Trans. Microwave Theory Tech.*, vol. 55, no. 12, pp. 2757–2765, Dec. 2007.

[24] Y. Yang, Y. Woo, J. Yi, and B. Kim, "A new empirical large-signal model of Si LDMOSFETs for high-power amplifier design," *IEEE Trans. Microwave Theory Tech.*, vol. 49, no. 9, pp. 1626–1633, Sept. 2001.

[25] W. H. Doherty, "A new high efficiency power amplifier for modulated waves," *Proc. IRE*, vol. 24, no. 9, pp. 1163–1182, Sept. 1936.

[26] Y. Yang, J. Yi, Y. Y. Woo, and B. Kim, "Optimum design for linearity and efficiency of microwave Doherty amplifier using a new load matching technique," *Microwave J.*, vol. 44, no. 12, pp. 20–36, Dec. 2001.

[27] F. H. Raab, "Efficiency of Doherty RF power-amplifier systems," *IEEE Trans. Broadcast.*, vol. BC-33, no. 3, pp. 77–83, Sept. 1987.

[28] J. Kim, J. Moon, B. Kim, and R. S. Pengelly, "A saturated PA with high efficiency," *IEEE Microwave Mag.*, vol. 10, no. 1, pp. 126–133, Feb. 2009.